NUKLEONIKA 2013;58(1):159–163

ORIGINAL PAPER

Characterization of phase constitution and magnetic properties of the hard magnetic nanocrystalline $Nd_{9.5}Fe_{63.65}B_{21.85}Nb_5$ alloy ribbons

Małgorzata Szwaja, Katarzyna Pawlik, Jerzy J. Wysłocki, Piotr Pawlik, Piotr Gębara

Abstract. In order to investigate the phase constitution of the nanocrystalline $Nd_{9.5}Fe_{63.65}B_{21.85}Nb_5$ alloy ribbons in the as-cast state and after short-time annealing Mössbauer study has been carried out. In as-cast state, ribbon samples were not fully amorphous but revealed soft magnetic properties. X-ray diffraction analysis showed the presence of hard magnetic $Nd_2Fe_{14}B$, metastable $Nd_2Fe_{23}B_3$ and paramagnetic $Nd_{1+\varepsilon}Fe_4B_4$ phases in annealed samples. Mössbauer spectroscopy was used to determine the fractions of constituent phases formed during annealing of ribbons. Magnetic measurements were made with a vibrating sample magnetometer (VSM) and have shown that with increasing annealing temperature the remanence polarization J_r and maximum energy product $(BH)_{max}$ values were increasing.

Key words: magnetic properties NdFeB alloys • nanocrystalline ribbon • $Nd_2Fe_{14}B$ • X-ray diffractometry

M. Szwaja✉, K. Pawlik, J. J. Wysłocki, P. Pawlik, P. Gębara
Częstochowa University of Technology,
Institute of Physics,
Department of Materials Processing Technology and Applied Physics,
19 Armii Krajowej Ave., 42-200 Częstochowa, Poland,
Tel./Fax: +48 34 325 0795,
E-mail: mszwaja@wip.pcz.pl

Received: 11 June 2012
Accepted: 14 September 2012

Introduction

Recently, there has been a great increase of interest in the study of phase constitution and magnetic properties of the Nd-Fe-B alloys doped with Nb, with a high content of boron [7, 10]. It has been shown that an admixture of the alloys with niobium retards grain growth and facilitates the formation of a more perfect nanocrystalline structure, which favors an increase in the coercivity [4]. In our previous works [5, 6], we have studied the phase constitution and magnetic properties of melt-spun $(Nd_{10}Fe_{67}B_{23})_{100-x}Nb_x$ alloys (where x = 1, 2, 3, 4) in the form of ribbons. Heat treatment led to nucleation and growth of the hard magnetic $Nd_2Fe_{14}B$, paramagnetic $Nd_{\varepsilon+1}Fe_4B_4$ and metastable $Nd_2Fe_{23}B_3$ phases.

In the present work combined XRD and Mössbauer spectroscopy studies of the ribbon samples containing 5 at.% of Nb are presented. Furthermore, the influence of annealing conditions on phase constitution and magnetic properties is discussed.

Experimental

Base alloy with nominal composition of $Nd_{9.5}Fe_{63.65}B_{21.85}Nb_5$ was produced from the high purity elements and pre-alloyed Fe-B of known composition by arc-melting under an Ar atmosphere. Samples were re-melted several times in order to get better homogenization. Subsequently, ribbons were produced by the melt spinning

technique under the Ar atmosphere at a linear speed of the copper roll surface of 35 m/s. The samples were annealed at various temperatures from 923 K to 1063 K for 5 min under protective argon atmosphere.

X-ray diffractometry (XRD) and Mössbauer spectroscopy were used to determine phase composition of the samples. The XRD patterns were measured using CuKα radiation. Transmission Mössbauer spectra were obtained using a constant acceleration spectrometer which utilized a rhodium matrix Co^{57} source and was calibrated at room temperature with an α-Fe foil. The Mössbauer spectra analysis was carried out using the Normos software. The estimated errors of the hyperfine parameters were at most: ±0.1 T for hyperfine fields (B_{hf}), ±0.02 mm/s for isomer shifts (IS) and ±0.05 mm/s for quadrupole splitting (QS). Weight percentage was calculated assuming equal recoil free fractions for all structural sites based on the known sample stoichiometry. In calculation the abundance of Fe atoms in the constituent phases was taken into account. Room temperature hysteresis loops were measured with a LakeShore 7307 vibrating sample magnetometer at external magnetic field up to 2 T.

Results and discussion

The phase constitution of the nanocrystalline $Nd_{9.5}Fe_{63.65}B_{21.85}Nb_5$ alloy ribbons in the as-cast state and annealed at various temperatures from 923 K to 1063 K for 5 min was determined from X-ray diffraction data. The selected XRD patterns are presented in Fig. 1.

The X-ray diffractions obtained for the alloy ribbon sample in the as-cast state (Fig. 1) consists of wide bump corresponding to the amorphous phase and superimposed numerous low intensity peaks related to precipitates of crystalline phases. However, small intensity of these peaks in comparison with the level of background does not allow unambiguous identification of crystalline phases present in the samples. Annealing at 923 K and higher temperatures for 5 min, resulted in significant changes in the crystal structure of the material. The main crystalline phase observed in the investigated specimans was the hard magnetic $Nd_2Fe_{14}B$ having a tetragonal structure (space group *P*42/*mnm*) [2]. Additionally, the phase analysis indicated the presence of the paramagnetic $Nd_{1.1}Fe_4B_4$ [1, 8] and the soft magnetic $Nd_2Fe_{23}B_3$ phases represented by three Zeeman lines corresponding to magnetically non-equivalent positions of Fe atoms [1, 4, 8]. Furthermore, one can expect precipitates of the soft magnetic α-Fe phase. However, due to overlapping of XRD peaks positions its presence was not evident. In order to estimate the volume fractions of constituent phases and verify the presence of α-Fe, the Mössbauer spectra analysis was performed. In the fitting procedure the existence of $Nd_2Fe_{14}B$ phase was represented by six Zeeman lines corresponding to the magnetically non-equivalent Fe atom positions in the unit cell. Those sites in the Wyckoff notation are denoted as $16k_1$, $16k_2$, $8j_1$, $8j_2$, $4e$, $4c$. Relative intensities ratios of the corresponding sextets were set as 4:4:2:2:1:1. Furthermore, the paramagnetic $Nd_{1.1}Fe_4B_4$ phase was represented by one doublet. The soft magnetic $Nd_2Fe_{23}B_3$ phase was described by three sextets with a relative intensity ratio 1:1:1, that correspond to the three magnetically non-equivalent Fe atoms positions. Mössbauer spectra analysis was carried out for as-cast sample and annealed ribbons at temperatures for which the best magnetic properties were found. The Mössbauer spectrum of $Nd_{9.5}Fe_{63.65}B_{21.85}Nb_5$ alloy ribbons in the as-cast state is shown in Fig. 2.

Rough overview of the spectrum suggests the existence of large fractions of ferromagnetic disordered and paramagnetic phases. However, based on the XRD and magnetic studies, the precipitation of hard magnetic phase cannot be excluded. Therefore in the analysis a minor fraction of the $Nd_2Fe_{14}B$ was taken into account. The hyperfine parameters for this phase were adopted from the literature [3, 9]. Furthermore, the experimental data were fitted taking into account the presence of paramagnetic $Nd_{1.1}Fe_4B_4$ crystalline phases and an additional component corresponding to the continuous distribution of hyperfine fields. This continuous component is attributed to the presence of amorphous phase formed during rapid solidification of the alloy. This is also in agreement with XRD results. The calculated hyperfine parameters (B_{hf} – hyperfine field, IS – isomer shift, QS – quadrupole splitting)

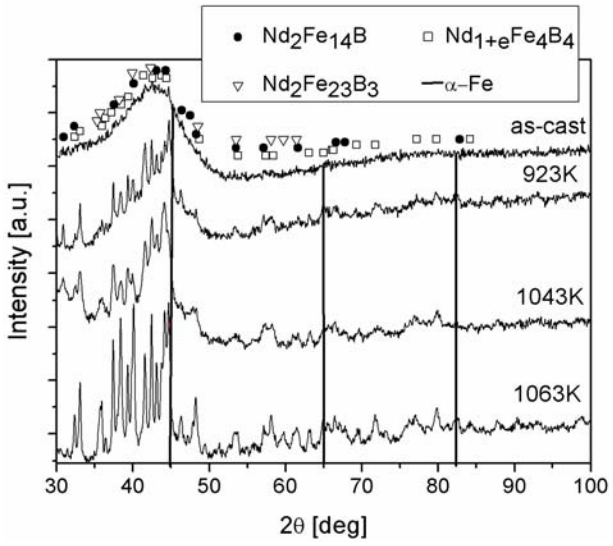

Fig. 1. X-ray diffraction patterns measured for $Nd_{9.5}Fe_{63.65}B_{21.85}Nb_5$ alloy ribbon samples in the as-cast state and annealed at 923, 1043 and 1063 K for 5 min.

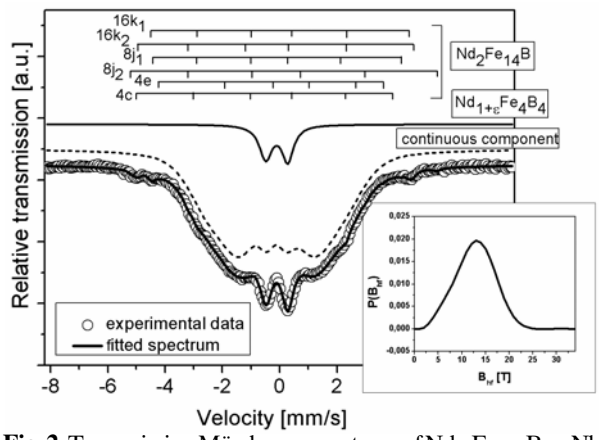

Fig. 2. Transmission Mössbauer spectrum of $Nd_{9.5}Fe_{63.65}B_{21.85}Nb_5$ alloy ribbon in the as-cast state with hyperfine field distribution for continuous component.

Table 1. The hyperfine parameters of the Mössbauer spectrum of $Nd_{9.5}Fe_{63.65}B_{21.85}Nb_5$ alloy ribbons in the as-cast state (B_{hf} – hyperfine field, IS – isomer shift, QS – quadrupole splitting, V – fractions of constituent phase)

As-cast $Nd_{9.5}Fe_{63.65}B_{21.86}Nb_5$		B_{hf} (T)	IS (mm/s)	QS (mm/s)	V (wt.%)
$Nd_2Fe_{14}B$ [3, 9]	16k_1	27.9	–0.12	0.30	3.5
	16k_2	29.8	–0.28	0.29	
	8j_1	26.8	–0.23	0.28	
	8j_2	33.1	0.03	0.27	
	4e	24.3	0.06	–0.67	
	4c	27.9	–0.44	–0.45	
$Nd_{1+\varepsilon}Fe_4B_4$		–	–0.09	0.77	11.1
Disordered phase		–	–	–	85.4

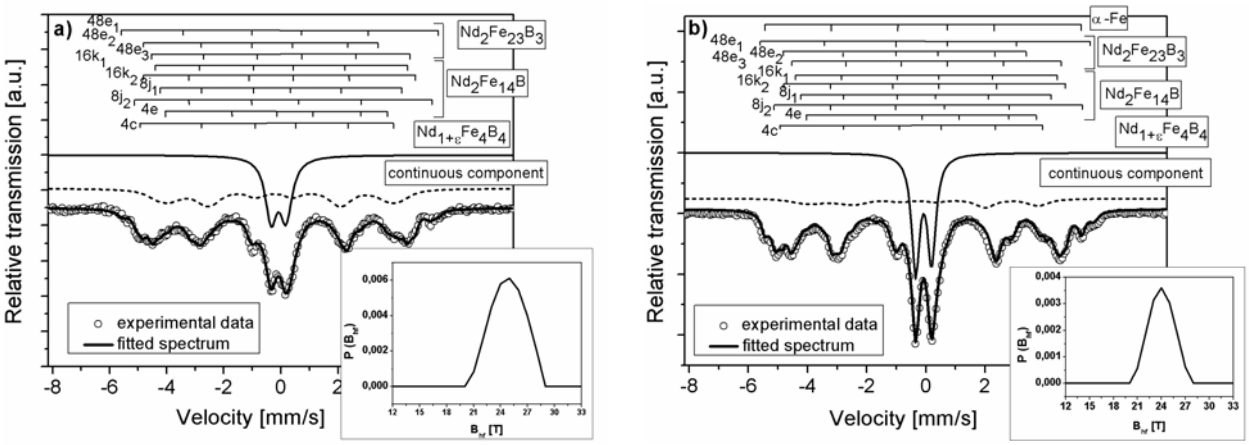

Fig. 3. Transmission Mössbauer spectra of $Nd_{9.5}Fe_{63.65}B_{21.85}Nb_5$ alloy ribbon annealed at 1043 K (a) and 1063 K (b) for 5 min with hyperfine field distribution for continuous component.

corresponding to the constituent phases of the as-cast ribbons were collected in Table 1.

It was shown that the majority of the sample consists of the amorphous phase (~85 wt.%). The rest of the fractions was occupied by the crystalline $Nd_2Fe_{14}B$ and $Nd_{1.1}Fe_4B_4$ phases. The Mössbauer spectra of $Nd_{9.5}Fe_{63.65}B_{21.85}Nb_5$ alloy ribbons annealed at 1043 K and 1063 K were shown in Fig. 3.

In the fitting procedure for the spectrum obtained for the ribbon annealed at 1043 K apart from $Nd_2Fe_{14}B$ and $Nd_{1.1}Fe_4B_4$ contributions, the additional three sextets were incorporated. These lines correspond to the $Nd_2Fe_{23}B_3$ phase. For the ribbons annealed at 1063 K a good fitting of calculated spectrum to the experimental data was achieved by taking into account the presence of α-Fe phase. The hyperfine parameters values obtained for the samples annealed at 1043 K and 1063 K are collected in Table 2.

It was shown that the hard magnetic and paramagnetic phases precipitated during rapid solidification (Fig. 2). The subsequent annealing resulted in evolution of the phase constitution. The volume fraction of both $Nd_2Fe_{14}B$ and $Nd_{1.1}Fe_4B_4$ phases rised with the annealing temperature in the expense of the disordered component. Furthermore, the $Nd_2Fe_{23}B_3$ phase was found during annealing. Additionally, the heat treatment at 1063 K resulted in formation of α-Fe. In case of disordered phase it was shown that the decrease of its volume fraction was accompanied by the shift of the maximum in the hyperfine field distribution towards higher fields.

Table 2. The hyperfine parameters of the Mössbauer spectrum of $Nd_{9.5}Fe_{63.65}B_{21.85}Nb_5$ alloy ribbons annealed at 1043 K and 1063 K (B_{hf} – hyperfine field, IS – isomer shift, QS – quadrupole splitting, V – fractions of constituent phase)

$Nd_{9.5}Fe_{63.65}B_{21.86}Nb_5$		B_{hf} (T)		IS (mm/s)		QS (mm/s)		V (wt.%)	
		1043 K	1063 K	1043 K	1063 K	1043 K	1063 K	1043 K	1063 K
$Nd_2Fe_{14}B$	16k_1	27.7	28.3	–0.16	–0.15	0.30	0.30	21.3	30.1
	16k_2	29.6	29.8	–0.22	–0.20	0.29	0.29		
	8j_1	26.1	26.8	–0.16	–0.11	0.28	0.28		
	8j_2	32.0	32.4	–0.05	–0.05	0.27	0.27		
	4e	23.8	24.3	0.20	0.25	–0.67	–0.67		
	4c	27.6	27.9	–0.38	–0.51	–0.35	–0.21		
$Nd_2Fe_{23}B_3$	48e_1	34.3	34.5	–0.10	–0.06	–0.15	0.40	9.1	11.7
	48e_2	27.2	28.3	–0.33	–0.33	–0.14	–0.28		
	48e_3	27.9	27.5	–0.04	–0.04	0.02	–0.07		
$Nd_{1+\varepsilon}Fe_4B_4$		–	–	–0.07	–0.07	0.53	0.55	40.2	42.6
α-Fe		–	33.1	–	–0.11	–	0.003	–	2.9
Disordered phase		–	–	–	–	–	–	29.4	12.7

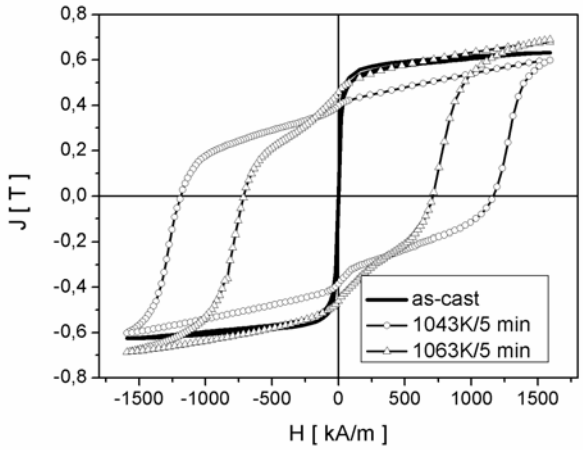

Fig. 4. The hysteresis loops measured for the $Nd_{9.5}Fe_{63.65}B_{21.85}Nb_5$ alloy ribbon samples in the as-cast state and annealed at 1043 and 1063 K for 5 min.

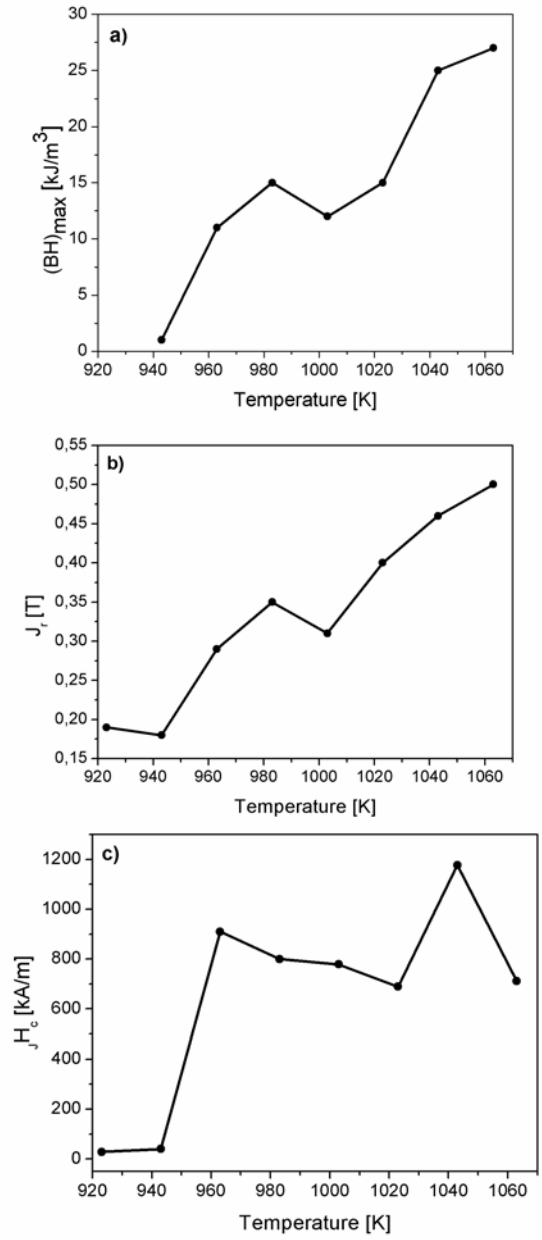

Fig. 5. The influence of annealing temperature on the maximum magnetic energy product $(BH)_{max}$ (a), remanence polarization J_r (b), coercivity field ${}_JH_c$ (c).

For all samples the measurements of magnetic hysteresis loops at room temperature were carried out. Selected hysteresis loops were presented in Fig. 4.

The evaluation of magnetic parameters values (maximum magnetic energy product $(BH)_{max}$, remanence polarization J_r, coercivity field ${}_JH_c$) with the annealing temperature was shown in Fig. 5.

The results of magnetic measurements showed soft magnetic properties of the as-cast sample. The changes of the shapes of hysteresis loops with the annealing temperature confirmed both the multiphase constitution of the samples and increase of the volume fraction of hard magnetic phase. The rise of annealing temperature resulted in the increase of the remanence polarization J_r from 0.19 T for 923 K to 0.50 T for 1063 K. The maximum value of the coercive field is achieved for the sample annealed at 1043 K and equals ${}_JH_c = 1176$ kA/m. The emerging of α-Fe phase seems to be advantageous for the remanence of the sample annealed at 1063 K. Gain in the remanence allowed to compensate the loss in coercivity for this sample that resulted in the highest $(BH)_{max}$ value of 27.4 kJ/m^3.

Conclusion

In the present work, the phase constitution and magnetic properties of the $Nd_{9.5}Fe_{63.65}B_{21.85}Nb_5$ alloy ribbons annealed at various temperatures from 923 K to 1063 K for 5 min were studied. It was found that the $Nd_{9.5}Fe_{63.65}B_{21.85}Nb_5$ alloy ribbon, produced by the free jet melt-spinning technique was not fully amorphous, however revealed soft magnetic properties. Heat treatment of these ribbons led to nucleation and growth of the hard magnetic $Nd_2Fe_{14}B$, paramagnetic $Nd_{1.1}Fe_4B_4$ and soft magnetic $Nd_2Fe_{23}B_3$ phases. Furthermore, the X-ray diffraction patterns obtained for the ribbons annealed at 1063 K shown the presence of additional peaks originating from the soft magnetic α-Fe phase. It was shown that the heat treatment leads to nanocrystalline structure of ribbon samples and good hard magnetic properties.

Acknowledgment. Work supported by the research project N N507 240840 financed by the Polish National Science Centre in the years 2011–2014.

References

1. Cheng Z, Shen B, Zhang J *et al.* (1997) Mössbauer spectroscopy and X-ray diffraction studies of the phase composition of crystallized $Nd_xFe_{81.5-x}B_{18.5}$ alloys with $7 \le x \le 15$. Chin Phys Lett 14;5:387–390
2. Herbst JF, Croat JJ, Pinkerton FE (1984) Relationships between crystal structure and magnetic properties in Nd2Fe12B. Phys Rev B 29;7:4176–4178
3. Pinkerton FE, Dunham WR (1984) Mössbauer effect studied of Nd2Fe14B and related melt-spun permanent magnet alloys. Appl Phys Lett 45;11:1248–1250
4. Popov AG, Serikov VV, Kleinerman NM (2010) Thermomagnetic and Mössbauer studies of structural transformations caused in the amorphous $Nd_9Fe_{85}B_5$ alloy by severe plastic deformation and annealing. Phys Met Metalloved 109;5:505–513

5. Szwaja M, Pawlik K, Wysłocki JJ, Gębara P (2011) Magnetic properties and phase constitution of the nanocrystalline $(Nd_{10}Fe_{67}B_{23})_{100-x}Nb_x$ (where x=1,2,3,4) alloy ribbons (abstract). Conf on Physics of Magnetism 2011 (PM'11), Poznań, Poland:161
6. Szwaja M, Pawlik P, Wysłocki JJ, Gębara P (2012) Magnetic properties of $Nd_{9.6}Fe_{64.32}Nb_4B_{22.08}$ alloy ribbons. Arch Metall Mater 57:233–236
7. Tamura R, Kobayashi S, Fukuzaki T, Isobe M, Ueda Y (2009) Synthesis and magnetic properties of Fe-B-Nd-Nb nanocomposite magnets. J Phys Conf Series 144:012068
8. Tilijan N, Zák T, Stajić-Trošić J, Menushenkov V (2002) Microstructure, magnetic properties and thermal stability of melt-spun Nd-Fe-B magnets with low Nd content. Metalurgija-Journal of Metallurgy 8:201–206
9. Yamasaki M, Hamano M, Kobayashi T (2002) Mössbauer study on the crystallization process of α-Fe/$Nd_2Fe_{14}B$ type nanocomposite magnet alloy. Mater Trans 43;11:2885–2889
10. Zhang J, Lim KY, Feng YP, Li Y (2007) Fe-Nd-B based hard magnets from bulk amorphus precursor. Scripta Mater 56: 943–946